Available online at www.sciencedirect.com
SCIENCE DIRECT®
Journal of Solid State Chemistry 178 (2005) 2751–2758
JOURNAL OF SOLID STATE CHEMISTRY
www.elsevier.com/locate/jssc

Preparation and physical properties of the solid solutions $Cu_{1+x}Mn_{1-x}O_2$ $(0 \leqslant x \leqslant 0.2)$

M. Trari[a], J. Töpfer[b], P. Dordor[c], J.C. Grenier[c], M. Pouchard[c], J.P. Doumerc[c,*]

[a]*Laboratoire de Stockage et de Valorisation des Energies Renouvelables, USTHB BP 32, El-Alia Algiers 16111 Algeria*
[b]*Fachhochschule Jena, FB SciTec Carl-Zeiss-Promenade 2, 07745 Jena, Germany*
[c]*Institut de la Matière Condensée de Bordeaux, ICMCB-CNRS, 87, avenue du Dr. Schweitzer, 33608 Pessac, Cedex, France*

Received 28 April 2005; received in revised form 7 June 2005; accepted 11 June 2005
Available online 21 July 2005

Abstract

Solid solutions of formula $Cu_{1+x}Mn_{1-x}O_2$ $(0 \leqslant x \leqslant 0.2)$ were synthesized by solid state reaction in silica sealed tubes. They crystallize with the monoclinic crednerite structure (space group $C2/m$). The stability domain in air is quite narrow and a phase diagram is proposed and compared with previous results. Magnetic study confirmed the HS state of Mn^{3+} ions and revealed that the predominant interactions are antiferromagnetic. Their strength decreases with x, which can be ascribed to a dilution effect, and long-range 3D magnetic ordering observed for $CuMnO_2$, disappears for $x > 0.05$. The crednerite solid solutions are p-type semiconductors. Modeling the thermoelectric power behavior suggests that charge carriers are Cu^{2+} holes diffusing in Cu layers for small x values and Mn^{4+} holes diffusing in Mn layers for $x > 0.05$. For larger x values a saturation effect limits the charge carrier concentration.

Keywords: Crednerite; Magnetic properties; Thermoelectric power; Jahn–Teller effect; Manganese oxides.

1. Introduction

In the last years, there is a renewed interest for delafossite compounds of general formula $CuMO_2$, which mainly concerns either fundamental problems of physics such as frustrated magnetic interactions in triangular lattices [1,2] or the search of new materials such as transparent p-type conducting oxides [3–5] for integration into transparent electronic devices [6] or semiconductors for thermoelectric conversion [7]. In this context understanding the relationships between chemical composition, and, structural and electronic properties can be very helpful. In this scope we have investigated the case were M=Mn that differs from others. Actually, the crednerite $CuMnO_2$ does not exhibit exactly the same symmetry as regular delafossites, but it undergoes a cooperative monoclinic distortion originating from the Jahn-Teller (JT) effect typical of Mn^{3+} ions. In fact, the C_{3v} distortion of the delafossite octahedrons does not match well the d^4 electronic configuration of Mn^{3+} as it does not lift the degeneracy of the e_g orbitals. The case of stoichiometric $CuMnO_2$ was previously considered from structural [8] as well as magnetic [9] point of view. In the present paper we extend the study to compositions richer in copper.

Previous studies of the system Cu–Mn–O are somewhat ambiguous and even contradictory. Rosenberg et al. [10] investigated this system between 850 and 1100 °C in air. They reported that the phases formed from various mixtures of CuO and Mn_2O_3 were CuO, Cu_2O, Mn_2O_3 (below 900 °C), hausmannite Mn_3O_4 (above 900 °C), a distorted tetragonal spinel $Cu_xMn_{3-x}O_4$ $(0 < x < 0.1)$, the cubic spinel $CuMn_2O_4$ and the monoclinic crednerite $CuMnO_2$ only above 900 °C.

*Corresponding author. Fax: +33 5 4000 8373.
E-mail address: doumerc@icmcb-bordeaux.cnrs.fr (J.P. Doumerc).

0022-4596/$ - see front matter © 2005 Elsevier Inc. All rights reserved.
doi:10.1016/j.jssc.2005.06.009

Schmall and Müller mentioned the compound $Cu_{1+x}Mn_{1-x-\delta}O_{2+\delta}$ ($x = 0.06$ and $\delta = 0.048$) [11]. Driessens and Rieck have extended the temperature range investigating the interaction of CuO and MnO oxides in air between 750 and 1400 °C [12]. In addition to the phases cited above the authors reported on a solid solution $Cu_{1+x}Mn_{1-x}O_2$ having a crednerite structure for $0 \leqslant x \leqslant 0.06$ and a delafossite structure for $0.08 \leqslant x \leqslant 0.12$. In order to clarify the situation and study its electronic properties we have prepared and characterized the solid solution $Cu_{1+x}Mn_{1-x}O_2$. The present paper summarizes and discusses the obtained results.

2. Experimental conditions

Samples with nominal compositions $Cu_{1+x}Mn_{1-x}O_2$ were prepared by direct solid state reaction ($0 \leqslant x \leqslant 0.20$) or by metathesis reaction ($x = 0$).

2.1. Solid state reaction

Solid state reactions were carried out according to one of the following equations depending whether the samples were heated in air or in sealed silica tubes:

$$(1+x)\ CuO + (1-x)/2\ Mn_2O_3 \rightarrow Cu_{1+x}Mn_{1-x}O_2 + (1-x)/4\ O_2\uparrow \quad (1)$$

$$(1-x)/2\ Cu + (1+3x)/2\ CuO + (1-x)/2\ Mn_2O_3 \rightarrow Cu_{1+x}Mn_{1-x}O_2 \quad (2)$$

In both cases, stoichiometric amounts of dried starting oxides were mixed in an agate mortar to ensure homogeneity, and pressed into pellets.

For reaction (1) heating was performed in air at 1050 °C in alumina boats for 24 h whereas for reaction (2) the mixture was fired in evacuated silica tubes at temperatures ranging from 960 °C for $x = 0$ to 1020 °C for $x = 0.2$. In both cases, samples were rapidly cooled down to room temperature. Generally, two grindings and firings were required to achieve complete reactions and well crystallized products.

Powder X-ray diffraction (XRD) patterns were obtained using a Phillips 1050 diffractometer with filtered Cu $K\alpha$ radiation. The lattice constants were refined by a least-square method from d-values determined using Si as calibration standard.

Electrical conductivity σ was measured on 8 mm-diameter discs sintered at the same temperature as that of the preparation (compactness ~70%) using a four probe technique. The thermoelectric power α was determined with an equipment described elsewhere [13].

Magnetic susceptibility was measured with a Manics DSM 8 type susceptometer.

3. Results and discussion

3.1. XRD study

For $0 \leqslant x \leqslant 0.2$, powder XRD spectra of $Cu_{1+x}Mn_{1-x}O_2$ samples prepared in sealed tubes show single phase products. They were indexed using a monoclinic unit cell (space group $C2/m$). For $CuMnO_2$ lattice constants are in good agreement with previous studies (Table 1).

For $x \geqslant 0.2$, the limiting phase $Cu_{1.2}Mn_{0.8}O_2$ coexists with the oxides Mn_2O_3, CuO and Cu_2O.

For preparations carried out in air, the reaction product compositions are reported in Table 2.

In the crednerite $CuMnO_2$, Mn and Cu atoms occupy the $2a$ (000) and $2d$ (01/21/2) positions of the space group $C2/m$, respectively. Oxygen atoms occupy the 4i positions of coordinates $x\,0\,y$. A drawing of the structure is given in Fig. 1. This strongly anisotropic structure is related to the delafossite, which can be described as a close packing of $(O–Cu–O)^{3-}$ dumbbells parallel to the c-axis of the delafossite hexagonal cell. Octahedral sites formed between two adjacent oxygen layers are occupied by Mn^{3+} ions. The monoclinic distortion of the crednerite can be ascribed to the cooperative JT effect of the Mn^{3+}-ions. All the octahedra are elongated in the same direction giving rise to an orbital ordering between the occupied d_z^2 orbitals directed along the elongated Mn–O bonds and

Table 1
Lattice constants and density of $CuMnO_2$. comparison with previous data

	Lattice constants				Density ($g\,cm^{-1}$)	
	a (Å)	b (Å)	c (Å)	β(°)	exp.	calc.
Direct solid state reaction	5.596	2.888	5.899	104.02	5.32	5.40
Metathesis reaction	5.596	2.884	5.890	103.94	5.28	5.41
McAndrew[a]	5.580	2.877	5.875	104	5.34	5.46
Kondrachev[b]	5.530	2.884	5.898	104.6	5.38	5.49

[a] J. McAndrew, Amer. Mineral. 41 (1956) 276.
[b] Yu.D. Kondrashev, Sov. Phys. Crystallogr. 3 (1958) 696.

Table 2
Compositions of reaction products for synthesis carried out in air

Nominal composition		Product compositions
$0 \leqslant x < 0.1$		$Cu_{1+x}Mn_{1-x}O_2$ (crednerite) + $Cu_yMn_{3-y}O_4$ (spinel)
$0.1 \leqslant x \leqslant 0.13$		$Cu_{1+x}Mn_{1-x}O_2$ (crednerite)
$0.13 < x \leqslant 0.20$	$T < 1030\,^{\circ}C$	$Cu_{1+x}Mn_{1-x}O_2$ (crednerite) + CuO
	$T > 1030\,^{\circ}C$	$Cu_{1+x}Mn_{1-x}O_2$ (crednerite) + Cu_2O

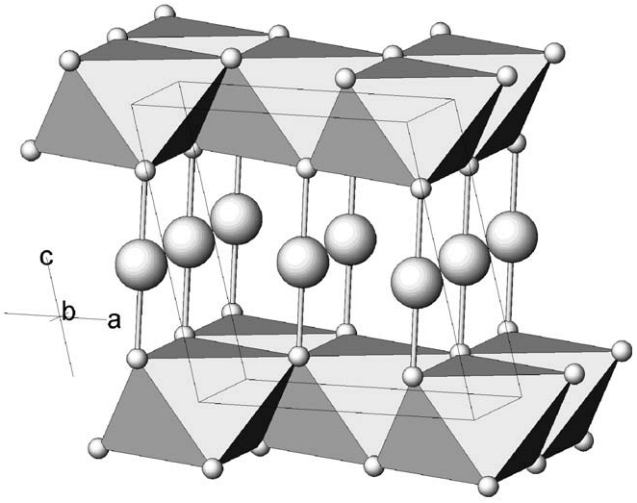

Fig. 1. Structure of the crednerite $CuMnO_2$.

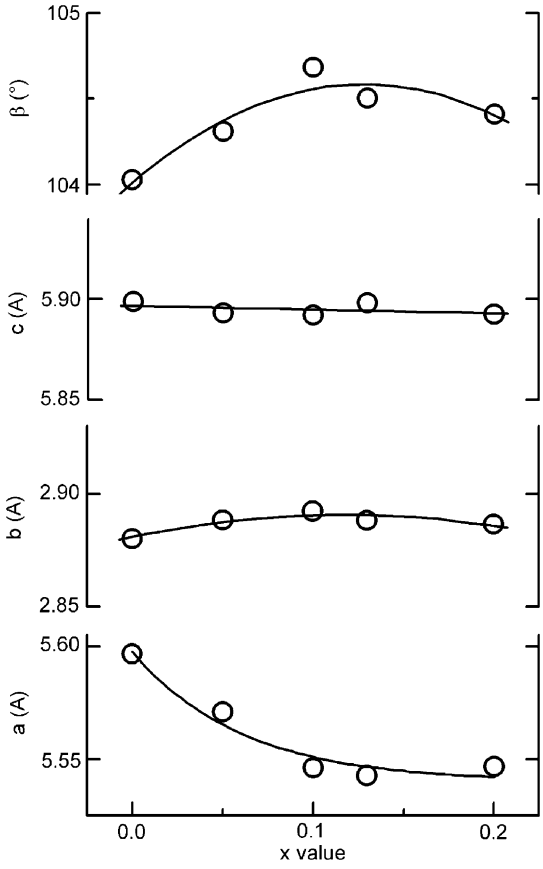

Fig. 2. Composition dependence of $Cu_{1+x}Mn_{1-x}O_2$ lattice parameters.

the empty $d_{x^2-y^2}$ orbitals directed towards the four closer oxygen atoms. Of course, this distortion removes the three fold axis characteristic of the flattened octahedrons of the parent delafossite structure.

Driessens and Rieck [12] had reported that $Cu_{1.13}Mn_{0.87}O_2$ underwent a martensitic transition from the crednerite form into a low-temperature delafossite form, near 1060 °C However, a XRD study that we have carried out as a function of temperature did not confirm this result.

The a constant of the monoclinic cell slightly decreases with x whereas the β angle slightly increases (Fig. 2). Both b and c parameters remain nearly constant. Such a behavior can simply result from the weak difference between the ionic radius of Mn^{3+} ($r^{3+}_{Mn} = 0.0645$ nm) and the average ionic radius ($r = 0.063$ nm) that can be attributed to a Mn^{4+}/Cu^{2+} pair ($r^{4+}_{Mn} = 0.053$ nm and $r^{2+}_{Cu} = 0.073$ nm).

3.2. Thermal stability of $Cu_{1+x}Mn_{1-x}O_2$

In air, TGA of $CuMnO_2$ shows a weight uptake above 400 °C (Fig. 3) that corresponds to the beginning of the reaction:

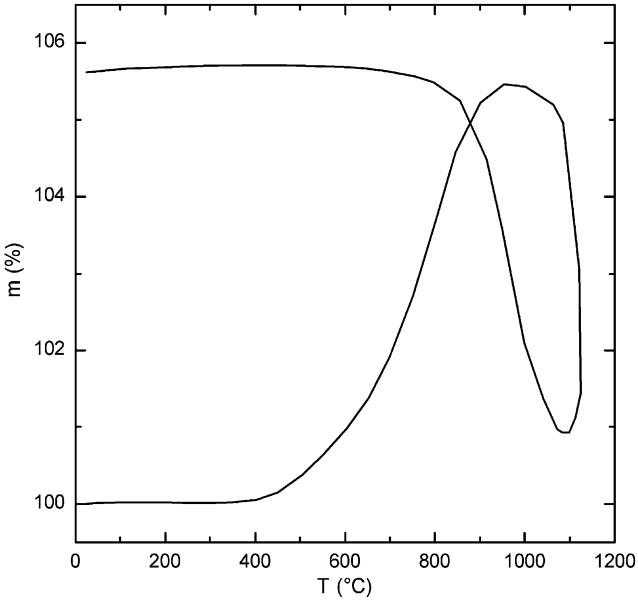

Fig. 3. TGA of $CuMnO_2$ in air.

$$CuMnO_2 + 1/(2(3-y))\ O_2 \rightarrow 1/(3-y)\ Cu_yMn_{3-y}O_4 + (3-2y)/(3-y)\ CuO.$$

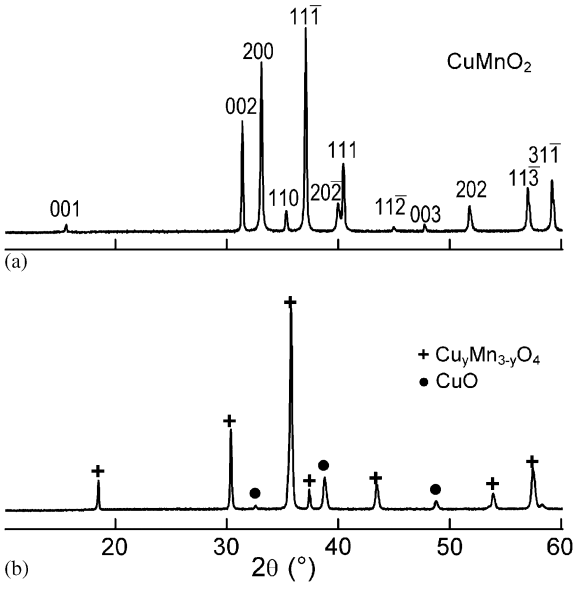

Fig. 4. XRD patterns of $CuMnO_2$ prepared in sealed tube (a) then heated in air at 800 °C (b) showing the decomposition into $Cu_yMn_{3-y}O_4$ ($1.05 < y < 1.5$) and CuO (see text).

This reaction is confirmed by XRD (Fig. 4). The maximum value of the relative mass increase ($\Delta m/m = 5.46\%$) is reached at 940 °C. It corresponds to the formation of the spinel $Cu_{1.05}Mn_{1.95}O_4$, which agrees with previous results concerning the composition range of spinels $Cu_yMn_{3-y}O_4$ [14].

Beyond 1080 °C, the sample weight steeply drops. Such a behavior can be attributed to the formation of the crednerite $Cu_{1+x}Mn_{1-x}O_2$ where the x-value should be close to 0.10 according to the XRD analysis of the products heated in air (Table 2). The reaction can be written as

$$1/(3-y)\ Cu_yMn_{3-y}O_4 + (3-2y)/(3-y)\ CuO \rightarrow \alpha\ Cu_{y'}Mn_{3-y'}O_4 + (2-3\alpha)/2\ Cu_{1+x}Mn_{1-x}O_2 + \{1/[2(3-y)] - \alpha/2\}O_2$$

with $\alpha = 2x/(3+3x-2y')$.

If we assume that the heating time at ca. 1080 °C is long enough to reach thermodynamic equilibrium, it is possible to determine the composition of one of the limiting phase from the observed weight loss, provided that the composition of the other one is known. Assuming that x is close to 0.1 as noticed above, yield a value of y' of about 0.5. This value is smaller than the one reported by Driessens and Rieck [12], but it is in good agreement with the one reported by Vandenberghe et al. [14]. It may be concluded from this study and from the conditions under which $CuMnO_2$ forms that the synthesis of this oxide requires oxygen partial pressures lower than 0.2 atm, in agreement with previously reported results [15].

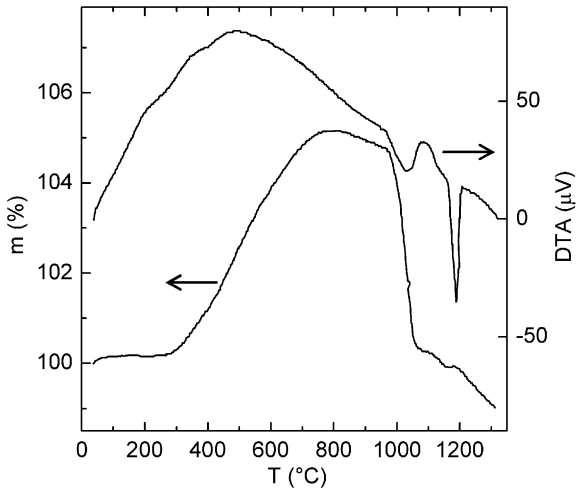

Fig. 5. Simultaneous TGA/DTA for $Cu_{1.1}Mn_{0.9}O_2$ in air (heating rate: $1.5^\circ\ mn^{-1}$).

The results of a simultaneous TGA/DTA study performed in air for $Cu_{1.1}Mn_{0.9}O_2$ are given in Fig. 5. The sample weight starts increasing near 320 °C and reaches a maximum value near 800 °C ($\Delta m/m = 5.18\%$). This exothermic oxidation can be written as:

$$Cu_{1.1}Mn_{0.9}O_2 + (1-x)/2(3-x)\ O_2 \rightarrow (1-x)/(3-x)\ Cu_xMn_{3-x}O_4 + (3+x)/(3-x)\ CuO.$$

On further heating, a continuous weight loss that is accompanied by an endothermic peak in the DTA curve, starts at 990 °C, then the sample recovers its initial mass at 1080 °C and reversibly converts back into a crednerite phase. The crednerite formation is denoted by an exothermic peak in the DTA curve. Beyond 1150 °C a weight loss is observed associated with an endothermic peak that corresponds to the incongruent melting of the sample:

$$Cu_{1+x}Mn_{1-x}O_2 \rightarrow Cu_{x'}Mn_{3-x'}O_4\ (\text{spinel}) + \text{liquid}.$$

These results as well as those of the synthesis (Table 2) lead to the phase diagram given in Fig. 6. They justify the sample quenching used for getting the crednerite at room temperature. The stability range of the crednerite solid solution $Cu_{1+x}Mn_{1-x}O_2$ is very narrow in air ($0.1 \leqslant x \leqslant 0.15$), but it is considerably extended when the oxygen partial pressure is reduced. Synthesis carried out in sealed tubes led to $0 \leqslant x \leqslant 0.2$.

3.3. Magnetic properties

The temperature dependence of the reciprocal magnetic susceptibility for $Cu_{1+x}Mn_{1-x}O_2$ ($x = 0, 0.05, 0.13, 0.20$) corrected for the diamagnetic contribution of core electrons [16] is given in Fig. 7 between 4 and 300 K. For $x \geqslant 0.05$, it tends to a Curie-Weiss behavior

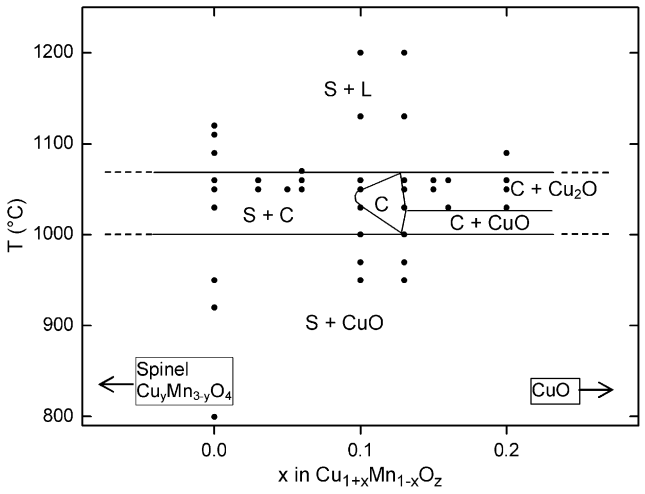

Fig. 6. Phase diagram for $Cu_{1+x}Mn_{1-x}O_2$ ($0<x<0.2$) in air (C = crednerite, S = spinel, L = liquid).

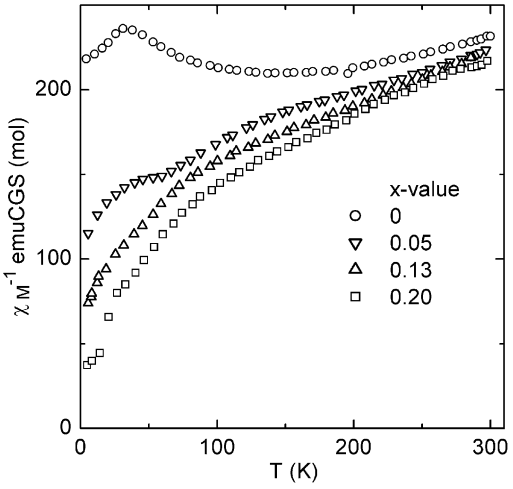

Fig. 7. Temperature dependence of the reciprocal molar magnetic susceptibility for $Cu_{1+x}Mn_{1-x}O_2$ solid solutions.

above ca. 150 K. The Curie constants are given in Table 3. Negative values of the Weiss constants θ_p denote the existence of dominant antiferromagnetic interactions.

As the temperature decreases the slope $d\chi^{-1}/dT$ decreases progressively, and, for $CuMnO_2$, the curve presents a broad minimum around 150 K typical of low-dimensional systems. A detailed study of the magnetic properties including a Mössbauer study of a ^{57}Fe-doped sample was reported elsewhere [9]. It showed that a 3D long–range magnetic ordering takes place below $T_N = 64$ K and that, as the temperature further decreases, a ferromagnetic component appears below 42 K, which corresponds to a peak in Fig. 7. A neutron diffraction study has revealed a complex magnetic structure [17].

Obviously, in $CuMnO_2$ copper is monovalent and manganese is trivalent that is confirmed by the value of the Curie constant although it is somewhat higher than the spin only value expected for HS Mn^{3+} (Table 3).

Table 3
Magnetic parameters of $Cu_{1+x}Mn_{1-x}O_2$

x-value	$C_{exp.}$	$C_{th.}$[a]			θ_p (K)
		$\varepsilon = 0$	$\varepsilon = x/2$	$\varepsilon = x$	
0	3.3	3.00	3.00	3.00	−450
0.05	3.2	2.81	2.85	2.89	−440
0.10	2.8	2.63	2.70	2.74	−430
0.13	2.4	2.51	2.60	2.71	−420
0.20	2.6	2.25	2.40	2.55	−330

[a] ε stands for the fraction of Cu^{2+} in A sites (see text).

For $x>0$ the electrical neutrality requires the formation of copper(II) and/or that of manganese(IV). Copper is distributed between two sublattices: the A–sublattice and the M–octahedral sites normally occupied by manganese in $CuMnO_2$, but which accommodate the copper excess. Of course, we shall assume that in octahedral sites copper is divalent. On the contrary, it is unlikely that a large amount of Cu^{2+} could occupy A-sites, but one cannot discard this hypothesis a priori. The oxide therefore is more accurately formulated as follows:

$$[Cu_{1-\varepsilon}{}^{+}\ Cu_{\varepsilon}{}^{2+}]_{A\ site}\ [Cu_{x}{}^{2+}\ Mn_{1-2x+\varepsilon}{}^{3+}\ Mn_{x-\varepsilon}{}^{4+}]_{B\ site}\ O_2 \quad (3)$$

In Table 3 are given calculated values of C_M for three values of ε (0, $x/2$, x) on the base of spin only contribution for all the ions. For Mn^{3+} and Mn^{4+} a HS state ($S = 2$ and 3/2, respectively) has been assumed. The variation of C_M with ε is too small for choosing between the three possibilities on the base of magnetic measurements only.

The negative and large absolute values of θ_p reveals the existence of strong antiferromagnetic interactions. The decrease of the absolute value of θ_p as x increases can normally be ascribed to a dilution effect as the number of magnetic nearest neighbors decreases. The 3D long range ordering observed for $CuMnO_2$ below 60 K as well as the weak ferromagnetic component observed below 42 K seems no longer exist for $x>0.05$. The vanishing of the broad minimum occurring in the $\chi^{-1} = f(T)$ curve near 150 K for $CuMnO_2$ can be attributed either to a shortening of the chains of manganese atoms [9] or to the existence of chains containing an odd number of spins.

3.4. Electrical properties

As the present investigation is carried out on sintered polycrystalline samples, the discussion of transport properties will mainly be confined to qualitative considerations. It is generally accepted that the thermoelectric power is less sensitive than the electrical

conductivity to grain boundary effects. On the other hand, on the base of structural considerations and of previous results on delafossite oxides we can assume that electronic transport is much easier within A or M atomic layers rather than along the c-axis and it contributes for a large part to the measured electric conductivity [18].

The temperature dependence of the electrical conductivity σ and that of the thermoelectric power α for $Cu_{1+x}Mn_{1-x}O_2$ solid solutions are given in Figs. 8 and 9, respectively. The data are limited on the low-temperature side by the large impedance of the samples.

These data clearly show that all the measured samples have an insulating (or semiconducting) behavior. This result agrees with the energy band diagram proposed by Rogers et al. for the AMO_2 delafossite [18].

The electrical conductivity follows an Arrhenius law for all the investigated samples: $\sigma = \sigma_0 \exp(-\Delta E/kT)$ (Fig. 8).

The activation energy of the electrical conductivity, ΔE is plotted vs. x in Fig. 10. This activation energy can correspond either (i) to the thermal creation of carriers by excitation across the band gap (intrinsic process) or by impurity ionization (extrinsic process), or to a thermal activation of the carrier mobility. The temperature dependence of the thermoelectric power discards the first possibility (i) as in such a case α should decrease with increasing T following a law of the type: $\alpha = (-k/e)(\Delta E/kT)$ whereas actually α remains practically constant in the whole investigated temperature range.

For charge carriers occupying a narrow band having a width of the order of kT or less, the thermopower is given by the Heikes relationship [19]:

$$\alpha = (-k/e)ln(1-c)/c \tag{4}$$

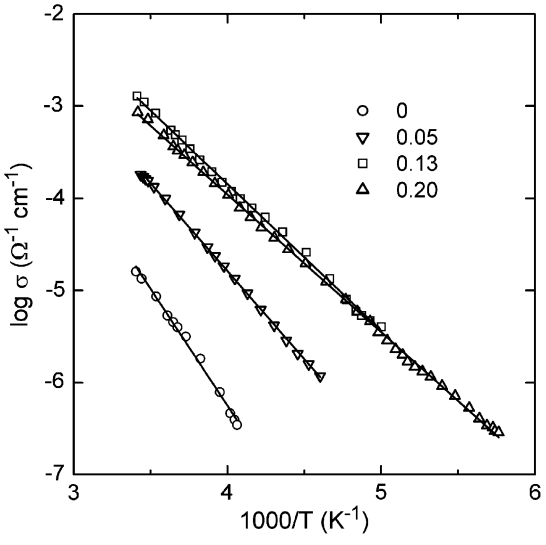

Fig. 8. Temperature dependence of the electrical conductivity plotted as log(σ) vs. T^{-1} for $Cu_{1+x}Mn_{1-x}O_2$ solid solutions.

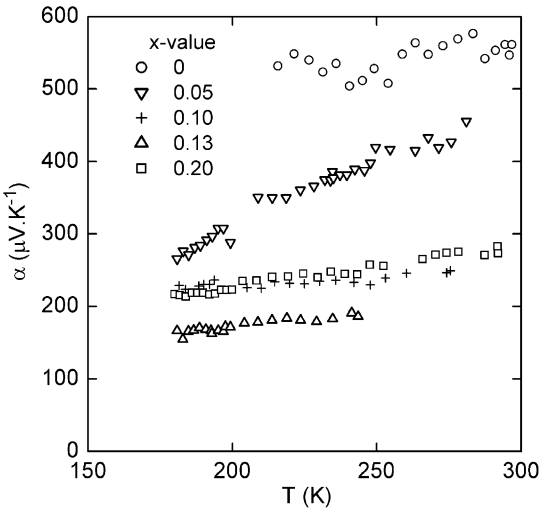

Fig. 9. Temperature dependence of the thermoelectric power for $Cu_{1+x}Mn_{1-x}O_2$ oxides.

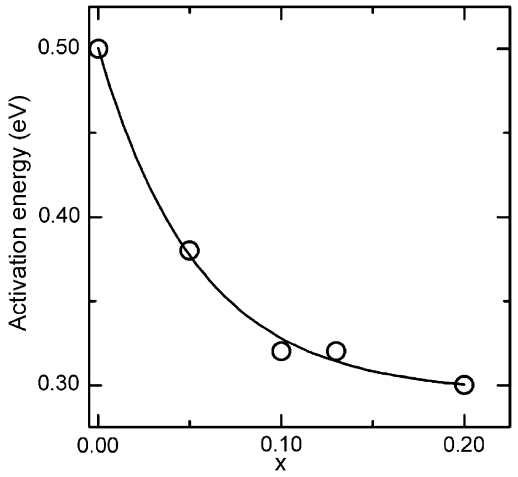

Fig. 10. Variation of activation energy for the electrical conductivity vs. x for $Cu_{1+x}Mn_{1-x}O_2$ solid solutions.

with $c = n/N$, where n is the number of electrons and N the number of available sites. About 30 years ago Chaikin and Beni have proposed to modify the Heikes formula in order to take into account the spin degeneracy in the evaluation of the entropy. The above relation (4) becomes

$$\alpha = (-k/e)\ln\ \beta(1-c)/c, \tag{5}$$

where $\beta = 2$ for electrons carrying a spin $S = 1/2$ and moving on a background of $S = 0$ holes.

About 10 years ago Doumerc pointed that Eqn. (5) does not give the same result for electrons and for holes or in other words that α does not vanish for a half filled band. He argued that for electrons hopping from a M^{n+} cation with spin S_e onto a $M^{(n+1)+}$ cation with spin S_h [20]:

$$\beta = (2S_e + 1)/(2S_h + 1). \tag{6}$$

For $S_e = 1/2$ and $S_h = 0$ the result of Chaikin and Beni is recovered.

More recently Marsh and Paris proposed also to take into account the orbital degeneracy [21].

For $Cu_{1+x}Mn_{1-x}O_2$ two kinds of holes should be considered: Cu^{2+} ions in A-sites and Mn^{4+} ions in octahedral M-sites as described by (3). In such a case, α is given by

$$\alpha = (\alpha_A\sigma_A + \alpha_M\sigma_M)/(\sigma_A + \sigma_M),$$

where σ_A and σ_M represent the contribution to the electrical conductivity of holes located in A- and M-sublattices, respectively. The terms α_A and α_M can be calculated from (5)

$$\alpha_A = (-k/e)\ln[\beta_A(1 - c_A)/c_A], \quad (7)$$

$$\alpha_M = (-k/e)\ln[\beta_M(1 - c_M)/c_M]. \quad (8)$$

The degeneracy terms β_A and β_M can be calculated using (6). For Cu^{2+} holes diffusing on a Cu^{+} network one obtains: $\beta_A = 1/2$. For Mn^{4+} ($S_h = 3/2$) ions distributed over a Mn^{3+} ($S_e = 2$) lattice $\beta_M = 5/4$, assuming a HS configuration for both type of ions.

Evaluating accurately c_A and c_M remains a real issue when applying Eqs. (7) and (8). For instance, potential fluctuations which can result from random distribution of cations can make some sites less stable than others and then reduce the number of available sites, N, whereas the carrier number, n, can be decreased by trapping. Neglecting these effects, c_A and c_M defined as the c quantity in (4) can be obtained using formula (3):

$$c_A = 1 - \varepsilon, \quad (9)$$

$$c_M = (1 - 2x + \varepsilon)/(1 - x). \quad (10)$$

Two limiting cases can be considered:

- hypothesis I: assuming $\sigma_A \gg \sigma_M$ and $\alpha_A\sigma_A \gg \alpha_M\sigma_M$,
- hypothesis II: assuming $\sigma_A << \sigma_M$ and $\alpha_A\sigma_A << \alpha_M\sigma_M$ in hypothesis I $\alpha \to \alpha_A$ while in hypothesis II $\alpha \to \alpha_M$

The values of the quantities ε and $(x-\varepsilon)$ defined in formula (3)—determined from room temperature α values using equations (7) to (10)—are given in Table 4 for both hypothesis.

Fig. 10 shows that the activation energy for hopping decreases significantly with x from $x = 0$ to $x = 0.1$ and then remains nearly constant for $x > 0.1$. This result suggests that predominant charge carriers are located in two different sublattices depending on the x-value. Holes are first created in a sublattice that we can label "sublattice I" where the hopping energy is large, then in another sublattice—"sublattice II"—where it is smaller. However, a saturation effect intervenes as the number of carriers cannot exceed some limit: actually, for $x > 0.1$, the electrical conductivity no longer increases (Fig. 8) and the thermoelectric power does not change much (Fig. 9). Looking at Table 4 leads us to identify sublattice I with the copper planes (A-sites) and sublattice II with the manganese layers (M-sites). Indeed, with hypothesis I, the obvious requirement $\varepsilon < x$ is not satisfied for $x = 0.10$ and 0.13. In addition, manganese(IV) has a strong tendency to oxidize Cu^{+} into Cu^{2+} and therefore the hole formation is first expected in A-sites. However, the concentration of Cu^{2+} is limited because of the two-fold coordination of copper: in fact, the existence of Cu^{2+} in the copper layers can be conceived only if it is associated with a proper site accommodation. For instance, one could imagine a shift of oxidized copper atoms from their normal positions (with a two-fold coordination) to a new position with a higher coordination e.g., a four-fold coordination. Another possibility is the insertion of oxygen atoms in the copper layers. Large amounts of oxygen can be inserted within the delafossite network as first demonstrated by Cava's group [22] and in Bordeaux [23] and structures of oxygen-rich phases were determined by Bordet's group [24]. However, large amounts of oxygen can be inserted only when the a lattice constant (the length of which is directly related to the size of the trivalent M element) is large enough like for rare earth, and the lower limit seems correspond to scandium [25]. The size of Mn^{3+} is then probably too small to allow a significant quantity of oxygen to enter the crednerite network. This was experimentally confirmed, at least within the limits of accuracy of chemical and structural analyses [26]. Anyway the difference of coordination between Cu^{+} and Cu^{2+} should lead to high values for the activation energy as it is experimentally observed for low x-values.

We have already pointed out that as x increased beyond a given value the concentration of charge carriers no longer grows. This is reflected in Table 4, for $x = 0.2$ under hypothesis II. The values shown there do not take into account such a saturation effect responsible for an incorrect evaluation of c_M. Actually, for $x = 0.2$ the high concentration of Cu^{2+} in the M layers should lead to the trapping of Mn^{4+} holes in the

Table 4
Values of the quantities ε and x-ε defined in formula (3) deduced from the thermoelectric power values taken at room temperature using Eqs. (7–8) and (9–10) in hypothesis I or II where the contribution of carriers in A-sites or M-sites is predominant, respectively

X	$\alpha_{exp.}$ (μVK^{-1})	hypothesis I		hypothesis II	
		ε	x-ε	ε	x-ε
0.00	550	0.0033	–	–	0.0013
0.05	430	0.013	0.037	0.045	0.005
0.10	240	0.11	–	0.058	0.042
0.13	180	0.20	–	0.052	0.078
0.20	250	0.10	0.10	0.166	0.034

vicinity of Cu^{2+} ions, in order to minimize the Coulomb energy of repulsion through octahedron common edges.

For $CuMnO_2$ ($x = 0$) charge carriers can be created by a slight departure from stoichiometry, undetectable by chemical analysis such as iodometric titration.

4. Conclusion

Using solid state reactions in silica sealed tubes, it was possible to synthesize solid solutions $Cu_{1+x}Mn_{1-x}O_2$ for $0 \leqslant x \leqslant 0.2$. They cristallize with the monoclinic crednerite structure (space group $C2/m$). For the purpose of comparison with previous results the stability domain was also investigated in air. It was found much narrower ($x < 0.13$) and the results are summarized in a local ($0 \leqslant x \leqslant 0.2$) phase diagram.

The study of magnetic behavior has confirmed that the electronic configuration of Mn^{3+} ions corresponds to a high spin state. Large negative Weiss constants have shown that the predominant interactions are strongly antiferromagnetic. Their strength decreases with x, which can ascribed to a dilution effect, and long-range 3D magnetic ordering observed for $CuMnO_2$, disappears for $x > 0.05$.

Electrical measurements have revealed that the crednerite solid solutions are p-type semiconductors and that the charge transport involves a hopping mechanism. The thermoelectric power behavior is discussed on the base of the Heikes model. The analysis suggests that charge carrier nature changes with composition: carriers are Cu^{2+} holes diffusing in Cu layers for small x values, but they mainly are Mn^{4+} holes diffusing in Mn layers for $x > 0.05$. As x further increases towards much larger values, the charge carrier concentration no longer grows. This saturation effect could be attributed to a coulomb trapping as the concentration of Cu^{2+} ions exceeds a certain threshold within the Mn-layers.

References

[1] M. Mekata, N. Yaguchi, T. Takagi, S. Mitsuda, H. Yoshizawa, J. Magn. Magn. Mater. 104–107 (1992) 823.
[2] P. Mendels, D. Bono, F. Bert, O. Garlea, C. Darie, P. Bordet, V. Brouet, M.-H. Julien, A.-D. Hillier, A. Amato, J. Phys.: Condens. Matter 16 (2004) S799–S804.
[3] H. Kawazoe, M. Yasukawa, H. Hyodo, M. Kurita, H. Yanagi, H. Hosono, Nature 389 (1997) 939.
[4] B.J. Ingram, G.B. González, T.O. Mason, D.Y. Shahriari, A. Barnabé, D. Ko, K.R. Poeppelmeier, Chem Mater 16 (2004) 5616.
[5] R. Nagarajan, N. Duan, M.K. Jayaraj, J. Li, K.A. Vanaja, A. Yokochi, A. Draeseke, J. Tate, A.W. Sleight, Int. J. Inorg. Mater. 3 (2001) 265–270.
[6] H. Kawazoe, H. Yanagi, K. Ueda, H. Hosono, MRS Bull 25 (2000) 28–36.
[7] K. Koumoto, H. Koduka, W.S. Seo, J. Mater. Chem. 11 (2001) 251.
[8] J. Töpfer, M. Trari, P. Gravereau, J.P. Chaminade, J.P. Doumerc, Z. Krist. 210 (1995) 184–187.
[9] J.P. Doumerc, M. Trari, J. Töpfer, L. Fournès, J.C. Grenier, M. Pouchard, P. Hagenmuller, Eur. J. Solid State Chem. 31 (1994) 705.
[10] M. Rosenberg, P. Nicolau, R. Manaila, P. Pausescu, Acad. Rep. Populare Romini Stud. Cercerati Fiz. 13 (1962) 651.
[11] V.N.G. Schmall, F. Müller, Z. Anorg. Allg. Chem. 332 (1964) 275.
[12] F.C.M. Driessens, G.D. Rieck, Z. Anorg. Allg. Chem. 351 (1967) 48.
[13] P. Dordor, E. Marquestaut, C. Salducci, P. Hagenmuller, Rev. Phys. Appl. 20 (1985) 795.
[14] R.D. Vanderberghe, C.G. Robbrecht, V.A.M. Brabers, Mater. Res. Bull. 8 (1973) 571.
[15] G. Rienäcker, K. Werner, Z. anorg. allg. Chem. 327 (1964) 275.
[16] E. König, in: Landolt-Börnstein (Ed.), vol. II, Springer, Berlin, New York, 1966, p. 16.
[17] J. Rodriguez-Carvajal, J.P. Doumerc, M. Trari, J. Töpfer, in preparation.
[18] D.B. Rogers, R.D. Shannon, C.T. Prewitt, J.L. Gillson, Inorg. Chem. 10 (4) (1971) 723.
[19] R.R. Heikes, J. Ure, Thermoelectricity, Interscience, New York, 1961.
[20] J.P. Doumerc, J. Solid State Chem. 110 (1994) 419.
[21] D.B. Marsh, P.E. Paris, Phys. Rev. B 54 (1996) 7720.
[22] R.J. Cava, H.W. Zandbergen, A.P. Ramirez, H. Takagi, C.T. Chen, J.J. Krajewski, W.F. Peck Jr., J.V. Waszczak, G. Meigs, R.S. Roth, L.F. Schneemeyer, J. Solid State Chem. 104 (1993) 437.
[23] M. Trari, J. Töpfer, J.P. Doumerc, M. Pouchard, A. Ammar, P. Hagenmuller, J. Solid State Chem. 111 (1994) 104.
[24] G. Van-Tendeloo, O. Garlea, C. Darie, C. Bougerol-Chaillout, P. Bordet, J. Solid State Chem. 156 (2001) 428.
[25] O. Garlea, P. Bordet, C. Darie, O. Isnard, R. Ballou, J. Phys. Condens. Mater. 16 (2004) 811.
[26] M. Trari, Thesis, University of Bordeaux 1, 1994.